Investigation of additively manufactured triply periodic minimal surfaces as an air-to-air heat exchanger

Alper Mete Genç [a,b], *Ceren Vatansever* [a], *Meltem Koçak* [b], *Ziya Haktan Karadeniz* [c].

[a] Graduate School of Natural and Applied Sciences, Izmir Kâtip Celebi University, Izmir, Turkey, alpergenc@eneko.com.tr.

[b] ENEKO, Cigli, Izmir, Turkey, meltemkocak@eneko.com.tr.

[c] Department of Energy Systems Engineering, Izmir Institute of Technology, Izmir, Turkey, haktankaradeniz@iyte.edu.tr.

Abstract. Additive manufacturing provides freedom of production and design of geometries that cannot be produced with traditional methods. Therefore high-efficiency and innovative heat exchanger designs can be produced with 3D printer technology efficaciously. Heat recovery ventilation devices, which meet the indoor air quality requirements with high thermal efficiency, allow heat recovery between the exhaust air and fresh air with the help of the recuperator, which is an air-to-air heat exchanger. In this study, the production processes of triply periodic minimal surfaces (TPMS) with the additive manufacturing method and their performance as an air-to-air heat exchanger are examined. Triply periodic minimal surfaces are three-dimensional and infinite surface geometries that can be expressed with continuous trigonometric functions, forming two separate non-intersecting spaces for fluids. The surface geometry derived from the trigonometric function can be arranged to provide heat transfer between two unmixed fluids at different temperatures. In this study, Schwarz-D, Schwarz-P and Shoen's gyroid geometries are investigated as triply periodic minimal surfaces. During the production of these geometries processes, parameters such as wall and layer thicknesses and printing temperature were changed to achieve the lowest possible wall thickness (0.16mm) with the 3D printer used. The performance of triply periodic minimal surface geometries as air-to-air heat exchangers are determined experimentally in a crossflow experimental setup.

Keywords. Heat exchanger, triply-periodic minimal surface, indoor air quality, additive manufacturing
DOI: https://doi.org/10.34641/clima.2022.172

1. Introduction

According to the International Energy Agency (IEA), world energy demand is incresing by 1.3% each year until 2040 (1). To reduce the increasing energy demand, studies are carried out to improve the energy efficiency of all systems used throughout the world. One of these systems is ventilation systems. Mechanical ventilation systems are now necessary for airtight buildings and are widely used in new residences and building restorations (2). These systems create a stable environment regarding thermal comfort and indoor air quality and create volumes where users can live healthily. The efficiency of ventilation systems depends on the accurate determination of the physiological needs of the users and the climatic variables, making the ventilation load calculations realistically and the correct operation of the systems. In addition, all ventilation system components should be designed to increase system efficiency and be in harmony with each other.

Heat exchangers, one of the most essential elements that significantly affect ventilation systems' energy efficiency and energy savings, are generally made of metal or ceramic materials. Heat exchangers are produced using traditional techniques such as machining or metal forming, which are today's engineering approaches. The efficiency that can be achieved with heat exchangers produced with traditional production technology is limited. This technology is far from flexible enough to meet an architect's aesthetic needs. The transformation created by the digital world we live in in the industry is discussed intensively with the concepts of "Digitalization" or "Industry 4.0". With Industry 4.0, the fourth industrial revolution, additive manufacturing is the latest move in smart automation technology. In this new era, the use of

modern production skills in the context of integrating new information technologies plays a vital role in economic competitiveness (3).

Because of its ability to create complex objects with advanced properties (new materials, shapes), additive manufacturing has become a key technology for producing customised products (4). Thanks to increased product quality, additive manufacturing is now used in various industries such as aerospace, biomedical, manufacturing and ventilation systems (5,6).

One of the basic geometries that can be used for an innovative start in heat exchanger design is the cellular structure family, triply periodic minimal surface (TPMS) porous structures, which consist of unit cells that can be repeated three-dimensionally to form lightweight, high-strength structures (7). The TPMS structures are investigated in a mechanical properties manner by Al-Ketan et al. (8). A comparison study is carried out by examining the topology-property relationship between 3D printed strut-based structures and several classes of TPMS structures. In an overall result, the diamond TPMS structure showed the best mechanical performance among all the tested structures. Abueidda et al. (9) studied three types of 3D printed TPMS structures experimentally and computationally to investigate the mechanical properties. It is found that the Neovius-CM and IPM-CM structures have a similar mechanical response and have higher stiffness and strength than Primitive-CM. TPMS structures are investigated variously along with mechanical properties. An analytical model is generated to investigate the permeability of TPMS structures, i.e., Fisher-Koch S, Gyroid and Schwarz P designs via Computational Fluid Dynamics (CFD) by Asbai-Ghoudan et al. (10). Results showed that the permeabilities of the three structures are increased with porosity at different rates. It is highlighted the importance of pore distribution and architecture. Besides these features that are investigated successfully, the thermal properties of TPMS structures are also studied in various studies. Catchpole-Smith et al. (11) show that the thermal conductivity of TPMS structures (Gyroid, Diamond Schwarz P) is primarily a function of the material properties and volume fraction sample. It is found that the Schwarz P geometry gave the highest conductivity among all the other structures which are manufactured by laser powder bed fusion. Cheng et al. (12) studied the morphology of TPMS structures which has a significant impact on fluid flow, heat/mass transport, and strength performance. Schwarz P, Schwarz D and Gyroid surfaces are investigated, resulting in the P structure having the lowest flow resistance and highest comprehensive heat transfer coefficient. Mechanical and thermal properties of TPMS structures are also investigated numerically to show the influence of geometric factors on the thermal and mechanical behaviour by Gawronska et al. (13). Cubic P, Diamond and Gyroid surfaces are simulated under load and heat transfer, resulting in that with an increasing number of cells, the effective stress values decrease. Considering the constant structure's volume, while the number of cells is increasing, it is shown that the usefulness of TPMS structures is successful.

Additionally, the high surface area to volume ratio is one of the biggest reasons these porous structures are among the potential heat exchanger feature geometry designs. Although the performance of these structures needs to be investigated in future studies, it is possible that they can provide a low-pressure drop with an increase in the surface area required for efficient heat transfer. Also, their large area/volume ratio, continuously bonded surface, inherent structural integrity, and good mixing potential make them suitable solutions for heat exchanger applications produced by additive manufacturing (14). The most studied variations of TPMS are diamond, primitive and gyroid structures, as mentioned. These structures have two separate areas that are continuous but not intersecting. With this feature, two independent channels can be provided. The fluid at two different temperatures can pass without mixing. It creates a structure that allows efficient use as a heat exchanger geometry in the air conditioning sector. Figure 1 shows the most well-known Schwarz P (Primitive), Schwarz D (Diamond) and Shoen's Gyroid TPMS surface models in the literature. Various studies have investigated TPMS structures as heat exchangers experimentally and numerically. Chandrasekaran (15) studied 3D printed Schwarz D geometry designed as heat exchangers experimentally. It is found that among heat exchangers with similar performance, the Schwarz D geometry is 32% smaller than a shell and tube heat exchangers in a manner of pressure drop. Schwarz D, P and Gyroid surfaces are investigated numerically via CFD analysis by Peng et al. (16). A numerical model is developed to optimise TPMS heat exchanger design parameters besides introducing a design workflow to present a streamline of fluid flows. Attarzadeh et al. (17) also studied the Schwarz D architecture by modelling to elucidate the design parameters and establish relationships between velocity, heat transfer and thermal performance at different wall thicknesses.

In this study, 3D printed Schwarz P, Schwarz D and Shoen's Gyroid surfaces are investigated experimentally to demonstrate a comparison between the geometries regarding performance parameters. Thermal efficiencies and pressure drops are obtained for the geometries at different flow rates and porosity ratios.

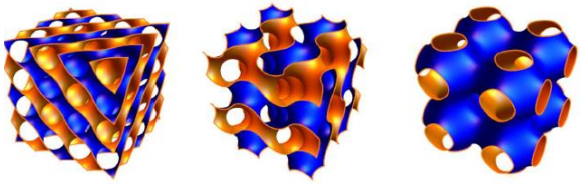

Fig. 1- Surface models of Schwarz D, Shoen's Gyroid and Schwarz P, respectively.

2. Material and method

In the current work, three different TPMS heat exchangers (Gyroid, Diamond and Primitive) with various wall thicknesses are created via Mathematica Programme according to equations 1, 2 and 3, respectively. Then, all geometries are exported. STL format and transferred to a 3-D printer. For each geometry (G, D and P), three different wall thicknesses were selected, and a total of nine heat exchangers were produced.

$$\cos(x)\sin(y) + \cos(y)\sin(z) + \cos(z)\sin(x) = 0 \quad (1)$$

$$\cos(x)\cos(y)\cos(z) - \sin(x)\sin(y)\sin(z) = 0 \quad (2)$$

$$\cos(x) + \cos(y) + \cos(z) = 0 \quad (3)$$

To obtain the thermal efficiency, each heat exchanger was put into the experimental setup, respectively. The experimental setup is shown in Figure 3 and the following assumptions have been considered:

- The inlet temperatures of the air to the system are 40 and 20°C for the hot and cold sides, respectively.
- The flow rate of the fluid is varied in a wide range, between 18 and 53 m^3/h.

In the subsections of material and method, additive manufacturing, pressure drop calculation, experimental setup and heat transfer efficiency have been mentioned.

2.1 additive manufacturing

Along with the fourth industrial revolution, namely Industry 4.0, is the recent movement on intelligent automation technology. In this new era, the utilisation of modern manufacturing skills such as additive manufacturing (AM) within the context of integrating novel information technologies plays a vital role in economic competitiveness [18]. Therefore, it is considered that additive manufacturing (AM) could become a key technology for producing customised products due to its ability to create complex objects with advanced attributes. (new materials, shapes) [18]. Thanks to increased product quality, AM is currently being used in various industries such as aerospace, biomedical, manufacturing and ventilation systems [19, 20]. AM has the potential to drastically change the way components for heat transfer are designed and manufactured [21]. AM provides flexibility to experiment with different complex designs that are otherwise difficult to manufacture with other traditional methods. In addition to advantages, it can reduce lead time such as fast prototyping, acceleration of R&D, on-time delivery of spare parts [22]. In general, AM is the process of building a 3-D object layer by layer. It helps us efficiently use the resources with reduced material waste compared to traditional methods [23]. Fused Deposition Modelling (FDM), Selective Laser Sintering (SLS) and Stereolithography (SLA) are the three 3-D printing techniques that are explored for their feasibility in manufacturing heat exchangers. For this study, FDM will be used to manufacture the heat exchangers because it is the cheaper and most used method to compare other 3-D printing options. FDM is a technology where the melt extrusion method is used to deposit filaments of thermal plastics according to a specific pattern. The layout for FDM consists of a printhead able to move along X and Y directions above a build platform. Nine different geometries, which are shown in Figure 2, were produced by the FDM 3-D printer. Each geometry is produced with a side of 114 mm to be placed in the experimental system. The porosity value of each geometry was obtained differently due to the different equations of TPMSs.

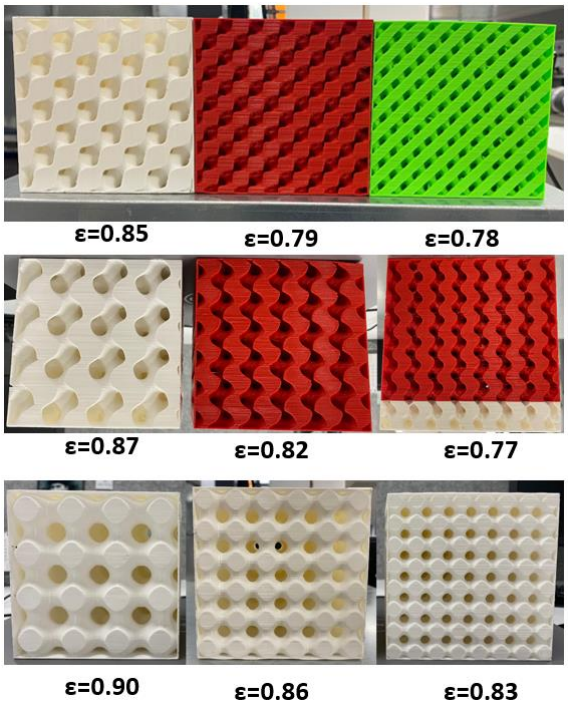

Fig. 2- TPMS heat exchangers produced via FDM

2.2 pressure drop

In the literature, there are several methods to calculate the pressure drop of porous media. One of these methods is presented by Fu et al. (2019) [24], who investigated hydrodynamic and mass transfer performances for three different TPMSs (G, D, P). The following equation is used to calculate the particle or pore diameter (d_p):

$$d_p = \frac{6(1-\varepsilon)}{a_p} \quad (4)$$

Here, ε represents the porosity or void ratio value. a_p is the specific area (m^2/m^3). The rearranged Re

number is as follows:

$$Re = \frac{\rho_G V_G d_P}{(1-\varepsilon)\mu_G} = \frac{3}{2}\frac{\rho_G V_G d_h}{\varepsilon \mu_G} \quad (5)$$

In equation 5, G represents the fluid properties. Also, d_h means the hydraulic diameter. It was stated that the Re number would be in the range of 0-2500, and the fluid velocity would be in the range of 0-3.5 m/s [24]. The pressure drop is calculated by equation 6:

$$\frac{\Delta P}{\Delta L} = \psi \frac{(1-\varepsilon)}{\varepsilon^3}\frac{F_v^2}{d_P} \quad (6)$$

The expression ψ is a resistance coefficient that comes from the Ergun equation (equation 7). F_v^2 represents the amount of pressure exerted by the fluid (equation 8):

$$\psi = \frac{150}{Re} + 1.75 \quad (7)$$

$$F_v = V_G\sqrt{\rho_G} \quad (8)$$

$$f = \frac{\Delta P}{\frac{1}{2}\rho V_g^2 \frac{L}{d_h}} \quad (9)$$

The friction factor (f) is shown in equation 9. Here, L is the length of the heat exchanger.

2.3 experimental setup

The experimental setup is designed to extract data to analyse the actual performance of the heat exchanger. The output of the experiments included four temperature measurements, T_{HI}, T_{CI}, T_{HO}, T_{CO}, flow rates on the hot and cold sides, and the differential pressure across the hot side of the heat exchanger.

A schematic diagram of the experimental setup for better understanding is in Figure 3. The volume flow rates in the experiment were regulated between 0.4 and 1.2 m/s. The temperatures are measured using calibrated Omega K-type thermocouple. These thermocouples can read temperatures up to 200°C. Thermocouples were placed into a small hole drilled in diameter of 6 mm deep into the pipe wall and fixed with thermally non-conductive goop paste. Through, thermocouples placed in the hot and cold airlines were not biased by the ambient temperature. The thermocouples are connected to an IMC STUDIO to record the required temperatures. The thermocouple wires are attached to the connector using hot glue to prevent any leakages. The thermal efficiency for the hot and cold fluid was calculated using the temperatures recorded during the experiments mentioned in chapter 5. We did not expect rapid temperature changes in the system, so the sampling rate was set at 1 S/s (samples/second). The software was developed with the help of Arduino to adjust the fluid velocities. This software has been transferred to an interface. The desired flow rates can be determined by changing the fan operating power. Flow rates can be measured via hotwire probes FTS07 immersed perpendicular to the flow.

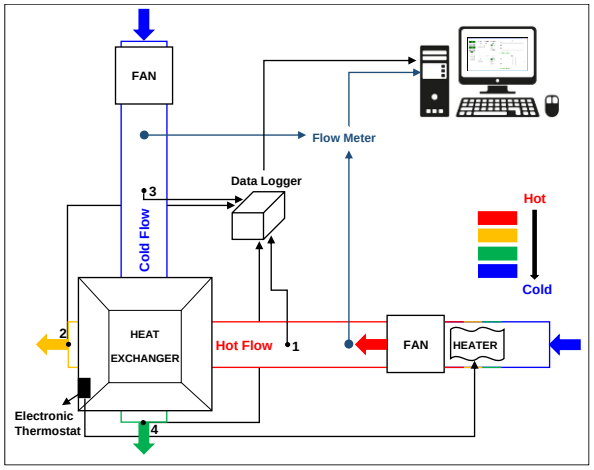

Fig. 3- A schematic diagram of the experimental setup

2.4 heat transfer efficiency

To analyse the experimental values, efficiency is calculated using the TS EN 308 standard [25]. The output of the experiments included 4 temperature measurements, T_{HI}, T_{CI}, T_{HO}, T_{CO}, flow rates on the hot and cold side, and the differential pressure across the hot side of the heat exchanger. The thermal efficiency can be calculated by using (equation 10):

$$\eta_t = \frac{T_{CO}-T_{CI}}{T_{HI}-T_{CI}} \quad (10)$$

In here;

T_{HI}: Hot air inlet temperature
T_{HO}: Hot air outlet temperature
T_{CI}: Cold air inlet temperature
T_{CO}: Cold air outlet temperature

3. Results and discussion

Firstly, internal and external leakage tests were carried out to control the leakage ratio in the system. External leakage tests were performed under 50, 75 and 100 Pa (Table 1). For all pressure values, external leakage ratios were obtained under %3. This means that there is no external leakage in our system.

Tab. 1 - External leakage ratios.

P_{stat} [Pa]	Leakage airflow [m^3/h]	Leakage ratio [%]
0	0	0.00
50	0.79	1.58
75	1.02	2.04
100	1.25	2.50

Internal leakage tests were carried out under 25, 50 Pa for all heat exchangers, and the obtained values are shown in Table 2 and 3, respectively.

Tab. 2 - Internal leakage ratios for 25 Pa.

Geometry	Leak. air flow [m³/h]	Leak. ratio [%]
Primitive(ε=0.90)	3.2	6.40
Primitive(ε=0.86)	3.7	7.40
Primitive(ε=0.83)	5.8	11.60
Diamond(ε=0.85)	2.8	5.60
Diamond(ε=0.79)	7.0	14.00
Diamond(ε=0.78)	15.9	31.80
Gyroid(ε=0.87)	1.6	3.20
Gyroid(ε=0.82)	2.5	5.00
Gyroid(ε=0.77)	4.3	8.60
No heat exch.	1.2	2.40

The internal leakage value is below 3% when a heat exchanger is not used under 25 Pa pressure. This shows no leakage in the system under 25 Pa pressure. The rate of internal leakage increases with the addition of heat exchangers to the system. For 25 Pa pressure, the highest internal leakage rate was obtained as 31.8% for Diamond(ε=0.78) geometry. When the tests performed under 50 Pa pressure are examined, the leakage rate for the without heat exchanger has increased and obtained as 6.4%. Also, among the heat exchangers, the leakage rate for the Diamond(ε=0.78) geometry increased to 66%.

Tab. 3 - Internal leakage ratios for 50 Pa.

Geometry	Leak. air flow [m³/h]	Leak. ratio [%]
Primitive(ε=0.90)	5	10.00
Primitive(ε=0.86)	5.6	11.20
Primitive(ε=0.83)	8.4	16.80
Diamond(ε=0.85)	5	10.00
Diamond(ε=0.79)	13.5	27.00
Diamond(ε=0.78)	33	66.00
Gyroid(ε=0.87)	3.2	6.40
Gyroid(ε=0.82)	11	22.00
Gyroid(ε=0.77)	33	66.00
No heat exch.	3.2	6.40

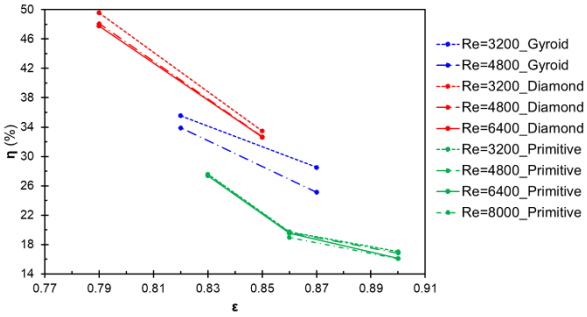

Fig. 4- Efficiency values against porosity

The heat transfer efficiency data are shown in Figure 4. The output of the experiments included four temperature measurements, T_{HI}, T_{CI}, T_{HO}, T_{CO}, flow rates on the hot and cold sides. Temperature values for Gyroid(ε=0.77), Diamond(ε=0.78) and Primitive(ε=0.83) geometries could not be obtained from hotwire probes because the system could not overcome the higher pressure drop. In addition, due to the stated reason, experiments at a Reynolds number of 8000 and 9600 for Diamond(ε=0.79) geometry, 6400, 8000 and 9600 for Gyroid(ε=0.82) geometry, and 9600 for Primitive(ε=0.83) geometry could not be performed. So, the efficiency could not be calculated due to this situation for these geometries. The highest efficiency is derived as approximately %50 for Diamond(ε=0.79) geometry.

Also, according to Figure 4, efficiency decreases with increasing porosity. The same is true for an increase in flow rate. As the flow rate increases, the efficiency decreases. The higher the leakage rate causes, the higher the efficiency due to the mixing of the cold and hot flows.

Pressure drops are calculated by the equations which are given in the pressure drop section. Then friction factor was calculated via pressure drop. Friction factor decreases with increasing Re number for all geometries, which are shown in Figures 5, 6 and 7 for Gyroid, Diamond and Primitive, respectively. Diamond geometries have a higher friction factor due to the more complex geometry compared to Gyroid and Primitive. So, Diamond geometries reach a higher pressure drop penalty with a lower Reynolds number regardless of porosity. Although Gyroid and Diamond have almost the same porosity (0.77 and 0.78, respectively), Diamond has a higher friction factor due to its complex geometry. The curve corresponding to Gyroid surfaces obtains the highest values of f for a given Re due to the dependency on dh factor. Diamond geometries have the lowest dh of the TPMS analysed and this results in a fluctuation of the friction factor values. Also, the friction factor increases with decreasing porosity and, the porosity decreases, the compactness also increases. This ensures the formation of a more rigid structure. On the other hand, increasing the compactness causes a higher friction factor. As a result, it is concluded that the structural integrity in the heat exchangers could not be fully achieved after additive manufacturing, and there are gaps in the exchangers. Heat exchangers need to be remanufactured and tested

using a different AM method such as SLS.

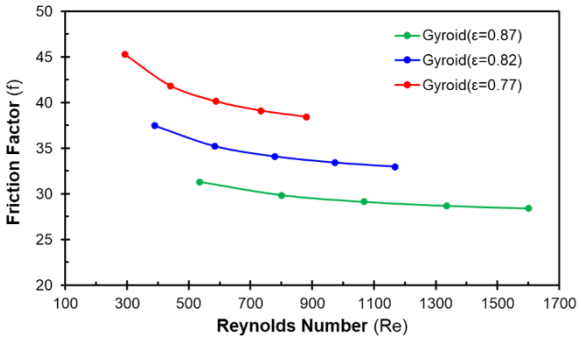

Fig. 5- Friction factor values for Gyroid geometries.

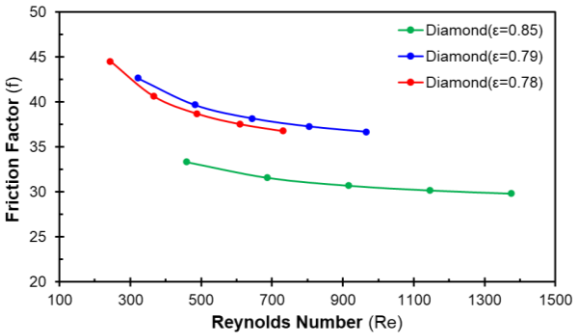

Fig. 6- Friction factor values for Diamond geometries.

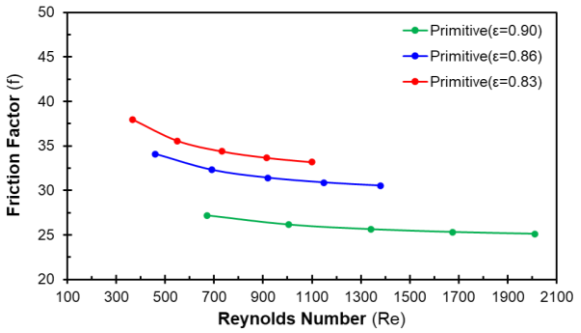

Fig. 7- Friction factor values for Primitive geometries.

4. Conclusion

In this study, 3D printed Schwarz P, Schwarz D and Shoen's Gyroid surfaces are investigated experimentally to demonstrate a comparison between the geometries regarding performance parameters. Thermal efficiencies, pressure drops and friction factors are obtained for the geometries at different flow rates and porosities.

The main conclusions are presented as follows:

- The highest efficiency is derived as approximately %50 for Diamon(ε=0.79) geometry.
- Temperature values for Gyroid(ε=0.77), Diamond(ε=0.78) and Primitive(ε=0.83) geometries could not be obtained from hotwire probes because the system could not overcome the higher pressure drop.
- Diamond geometries reach a higher pressure drop penalty with a lower Reynolds number regardless of porosity due to more complex geometry.
- Friction factor decreases with increasing Reynolds number regardless of TPMS geometries. Also, friction factor is inversely proportional to porosity.
- For all pressure values, external leakage ratios are obtained under %3. This means that there is no external leakage in the experimental system.
- Internal leakage ratios are obtained above %3. Since the structural integrity in the heat exchangers could not be fully achieved after additive manufacturing, and there are gaps in the exchangers. Heat exchangers need to be remanufactured and tested using a different AM method such as SLS.

As a future work, the experiments will be carried out by establishing a system that can overcome the pressure drop. Thus, thermal efficiency and pressure drop values will be obtained for a broader range of flow rates. Due to the gaps in the heat exchangers after additive manufacturing, geometries will be produced with a different additive manufacturing method. In this way, the actual efficiency of the heat exchangers will be obtained.

5. Acknowledgement

The authors would like to thank the anonymous reviewers for their careful reading of the manuscript and valuable suggestions for its improvement. Also, special thanks to Eneko Havalandırma ve Isı Ekonomisi Sistem Teknolojileri A.Ş. for their unwavering support in the use of the laboratory.

6. References

[1] IEA – International Energy Agency - IEA [Internet]. [cited 2022 Jan 10]. Available from: https://www.iea.org/reports/world-energy-outlook

[2] Natural Resources Canada [Internet]. [cited 2022 Jan 10]. Available from: https://www.nrcan.gc.ca/home

[3] Dilberoglu UM, Gharehpapagh B, Yaman U, Dolen M. The Role of Additive Manufacturing in the Era of Industry 4.0. Procedia Manufacturing. 2017 Jan 1;11:545–54.

[4] ASHRAE. Ventilation for Acceptable Indoor Air Quality, Standard 62.1. 2016.

[5] Ayar O, Yalçınkaya M, Karadeniz ZH, Gezgin E. Isı Geri Kazanımlı Havalandırma Cihazları İçin 3

Boyutlu Yazıcı ile Üretilebilecek Isı Değiştirici Tasarımı ve İmalatı. In: 13 Ulusal Tesisat Mühendisliği Kongresi. İzmir; 2017.

[6] Thompson MK, Moroni G, Vaneker T, Fadel G, Campbell RI, Gibson I, et al. Design for Additive Manufacturing: Trends, opportunities, considerations, and constraints. CIRP Annals. 2016;65(2):737–60.

[7] Panesar A, Abdi M, Hickman D, Ashcroft I. Strategies for functionally graded lattice structures derived using topology optimisation for Additive Manufacturing. Additive Manufacturing. 2018 Jan 1;19:81–94.

[8] Al-Ketan O, Rowshan R, Abu Al-Rub RK. Topology-mechanical property relationship of 3D printed strut, skeletal, and sheet based periodic metallic cellular materials. Additive Manufacturing. 2018 Jan;19:167–83.

[9] Abueidda DW, Bakir M, Abu Al-Rub RK, Bergström JS, Sobh NA, Jasiuk I. Mechanical properties of 3D printed polymeric cellular materials with triply periodic minimal surface architectures. Materials & Design. 2017 May;122:255–67.

[10] Asbai-Ghoudan R, Ruiz de Galarreta S, Rodriguez-Florez N. Analytical model for the prediction of permeability of triply periodic minimal surfaces. Journal of the Mechanical Behavior of Biomedical Materials. 2021 Dec;124:104804.

[11] Catchpole-Smith S, Sélo RRJ, Davis AW, Ashcroft IA, Tuck CJ, Clare A. Thermal conductivity of TPMS lattice structures manufactured via laser powder bed fusion. Additive Manufacturing. 2019 Dec;30:100846.

[12] Cheng Z, Xu R, Jiang P-X. Morphology, flow and heat transfer in triply periodic minimal surface based porous structures. International Journal of Heat and Mass Transfer. 2021 May;170:120902.

[13] Gawronska E, Dyja R. A Numerical Study of Geometry's Impact on the Thermal and Mechanical Properties of Periodic Surface Structures. Materials. 2021 Jan 16;14(2):427.

[14] Wadsö I, Holmqvist S. Additively Manufactured Heat Exchangers. [Lund, Sweden]; 2020.

[15] Chandrasekaran G. 3D Printed Heat Exchangers: An Experimental Study. 2018.

[16] Peng H, Gao F, Hu W. Design, Modelling and Characterization of Triply Periodic Minimal Surface Heat Exchangers with Additive Manufacturing. In: 30th Annual International Solid Freeform Fabrication Symposium. Texas-USA; 2019.

[17] Attarzadeh R, Rovira M, Duwig C. Design analysis of the "Schwartz D" based heat exchanger: A numerical study. International Journal of Heat and Mass Transfer. 2021 Oct;177:121415.

[13] Korsavi, S. S., Montazami, A., & Mumovic, D. (2020). Indoor air quality (IAQ) in naturally-ventilated primary schools in the UK: Occupant-related factors. Building and Environment, 106992.

[14] Pegas, P. N., Alves, C. A., Evtyugina, M. G., Nunes, T., Cerqueira, M., Franchi, M., ... & Freitas, M. C. (2011). Indoor air quality in elementary schools of Lisbon in spring. Environmental Geochemistry and Health, 33(5), 455-468.

[15] de Gennaro, G., Dambruoso, P. R., Loiotile, A. D., Di Gilio, A., Giungato, P., Tutino, M., ... & Porcelli, F. (2014). Indoor air quality in schools. Environmental chemistry letters, 12(4), 467-482.

[16] Bluyssen, P. M. (2017). Health, comfort and performance of children in classrooms–new directions for research. Indoor and Built Environment, 26(8), 1040-1050.

[17] Annesi-Maesano, I., Baiz, N., Banerjee, S., Rudnai, P., Rive, S., & SINPHONIE Group. (2013). Indoor air quality and sources in schools and related health effects. Journal of Toxicology and Environmental Health, Part B, 16(8), 491-550.

[18] Dilberoglu, U. M., Gharehpapagh, B., Yaman, U., & Dolen, M. (2017). The role of additive manufacturing in the era of industry 4.0. Procedia Manufacturing, 11, 545-554.

[19] Ayar, O., Yalçınkaya, M. A., Karadeniz, Z. H., Gezgin, E. 2017. "Isı Geri Kazanımlı Havalandırma Cihazları İçin 3 Boyutlu Yazıcı ile Üretilebilecek Isı Değiştirici Tasarımı ve İmalatı" 13. Ulusal Tesisat Mühendisliği Kongresi, 19-22 Nisan, İzmir.

[20] Thompson, M. K., Moroni, G., Vaneker, T., Fadel, G., Campbell, R. I., Gibson, I., ... & Martina, F., 2016. "Design for Additive Manufacturing: Trends, opportunities, considerations, and constraints", CIRP annals: manufacturing technology, 65(2), 737-760.

[21] Catchpole-Smith, S., Sélo, R. R. J., Davis, A. W., Ashcroft, I. A., Tuck, C. J., & Clare, A. (2019). Thermal conductivity of TPMS lattice structures manufactured via laser powder bed fusion. Additive Manufacturing, 30, 100846.

[22] Tirelli, V. (2020, May). Additive Manufacturing in Heat Exchangers and Valves. In Offshore Technology Conference. Offshore Technology Conference.

[23] Danayat, S. S. (2019). Investigating 3-D Printed Polymer Heat Exchanger (Doctoral dissertation, Arizona State University).

[24] Fu, Y., Bao, J., Wang, C., Singh, R. K., Xu, Z., & Panagakos, G. (2019). CFD Study of Countercurrent Flow in Triply Periodic Minimal Surfaces with CO2BOL Solvent (No. PNNL-29590). Pacific Northwest National Lab. (PNNL), Richland, WA (United States).

[25] TS EN 308: Isı eşanjörleri-Havadan havaya ve atık gazlardan ısı kazanımı cihazlarının performansının tayini için deney metotları, 1997.

Data Statement

The datasets generated during and/or analysed during the current study are not publicly available because they could be the subject of future works, but will be available the reason for the need can be requested from the corresponding author by specifying it.